BMC Plant Biology

RESEARCH Open Access

Transcriptomics and metabolomics analyses of *Rosa hybrida* to identify heat stress response genes and metabolite pathways

Hua Wang[1*], Wanting Xu[1], Xiaojuan Zhang[1], Lian Wang[1], Suqi Jia[1], Shuwei Zhao[1], Wan Li[1], Rongqianyi Lu[1], Aihua Ren[2] and Shuiming Zhang[1*]

Abstract

Background Global warming has greatly increased the impact of high temperatures on crops, resulting in reduced yields and increased mortality. This phenomenon is of significant importance to the rose flower industry because high-temperature stress leads to bud dormancy or even death, reducing ornamental value and incurring economic losses. Understanding the molecular mechanisms underlying the response and resistance of roses to high-temperature stress can serve as an important reference for cultivating high-temperature-stress-resistant roses.

Results To evaluate the impact of high temperatures on rose plants, we measured physiological indices in rose leaves following heat stress. Protein and chlorophyll contents were significantly decreased, whereas proline and malondialdehyde (MDA) contents, and peroxidase (POD) activity were increased. Subsequently, transcriptomics and metabolomics analyses identified 4,652 common differentially expressed genes (DEGs) and 57 common differentially abundant metabolites (DAMs) in rose plants from four groups. Enrichment analysis showed that DEGs and DAMs were primarily involved in the mitogen-activated protein kinases (MAPK) signaling pathway, plant hormone signal transduction, alpha-linolenic acid metabolism, phenylpropanoid biosynthesis, and flavonoid biosynthesis. The combined analysis of the DEGs and DAMs revealed that flavonoid biosynthesis pathway-related genes, such as *chalcone isomerase* (*CHI*), *shikimate O-hydroxycinnamoyl transferase* (*HCT*), *flavonol synthase* (*FLS*), and *bifunctional dihydroflavonol 4-reductase/flavanone 4-reductase* (*DFR*), were downregulated after heat stress. Moreover, in the MAPK signaling pathway, the expression of genes related to jasmonic acid exhibited a decrease, but *ethylene receptor* (*ETR/ERS*), *P-type Cu + transporter* (*RAN1*), *ethylene-insensitive protein 2/3* (*EIN2*), *ethylene-responsive transcription factor 1* (*ERF1*), and *basic endochitinase B* (*ChiB*), which are associated with the ethylene pathway, were mostly upregulated. Furthermore, heterologous overexpression of the heat stress-responsive gene *RcHSP70* increased resistance to heat stress in *Arabidopsis thaliana*.

Conclusion The results of this study indicated that the flavonoid biosynthesis pathway, MAPK signaling pathway, and plant hormones may be involved in high-temperature resistance in roses. Constitutive expression of *RcHSP70* may

*Correspondence:
Hua Wang
810690115@qq.com
Shuiming Zhang
zhangshuiming@ahau.edu.cn

Full list of author information is available at the end of the article

contribute to increasing high-temperature tolerance. This study provides new insights into the genes and metabolites induced in roses in response to high temperature, and the results provide a reference for analyzing the molecular mechanisms underlying resistance to heat stress in roses.

Keywords *Rosa hybrida*, Heat stress, Transcriptomics, Metabolomics

Background

Heat stress due to global warming poses a significant threat to food security and agricultural sustainability [1]. Elevated temperatures associated with heat stress can decrease water content, disrupt cellular homeostasis, and compromise vital biological processes [2]. These physiological disturbances can have devastating effects, leading to reduced crop yields and, in extreme cases, plant death [1]. *Rosa hybrida* is an important ornamental plant that grows and blooms at an optimum temperature of 22–26 °C. Roses are sensitive to high temperatures, which often decrease the number or size of flowers and cause them to enter dormancy and not blossom [3, 4].

Plants have evolved complex and diverse systems to cope with environmental heat stress [1, 2, 5]. At the molecular level, plants rely on transcriptional regulatory networks to orchestrate their stress responses. Heat shock proteins (HSPs) and reactive oxygen species (ROS) are major biomarkers of plant responses to heat stress [6–9]. The transcriptional regulatory network activated by heat stress is a highly dynamic and coordinated system. For instance, tomato and *Arabidopsis* heat shock transcription factor A1 (HsfA1) plays a critical role in the heat shock response by decreasing the induction of heat stress-responsive genes and heat stress-sensitive phenotypes [10, 11]. Among them, some genes encode proteins that protect cellular components from damage caused by heat stress, whereas others encode proteins that repair damage or restore cellular homeostasis [12–15].

In addition to transcriptional regulation, post-translational modifications play pivotal roles in the heat stress response of plants. These modifications, including phosphorylation [16], ubiquitination [17], and SUMOylation [18–20], can alter the activity, localization, or stability of proteins involved in stress signaling and responses. For instance, Ca^{2+} and ROS may be involved in heat stress sensing via MAPK signaling [21–23]. Moreover, plant hormones such as jasmonic acid play key roles in abiotic stress responses [24], and early signaling enhances heat tolerance in *Arabidopsis* [25]. In roses, Li et al. identified Ca^{2+} signaling pathways and transcription factors associated with rapid sensing and signal transduction in heat stress responses [4].

Researchers have extensively studied genes linked to regulatory pathways involved in heat stress. Ubiquitin E3 ligase (AtPUB48), HSP, heat-induced RING finger protein 1 (OsHIRP1), and drought, heat, and salt-induced RING finger protein 1 (OsDHSRP1) are involved in protein stability and refolding [26–29]. In particular, the relationship between HSP proteins and heat stress responses has been reported in several species [3, 11, 27, 30]. In addition, cyclic nucleotide-gated ion channel protein (CNGC) and calcium-dependent protein kinase (CDPK) play crucial roles in the response to high temperatures via Ca^{2+} signaling pathways [31–35]. Moreover, genes such as *WRKY39* in *Arabidopsis* and jasmonic acid 2 (*SlJA2*) in tomatoes respond to high temperatures by regulating salicylic acid (SA) signaling [36, 37]. In roses, eukaryotic translation initiation factor 5 A (RceIF5A) and APETALA2 were found to respond to high temperatures or temperature fluctuations [38, 39].

Despite these advances in the understanding of the molecular mechanisms underlying plant heat stress responses, the molecular mechanism underlying the response to heat stress in roses remains unknown. In this study, the "Francois Rabelais" rose variety was used and subjected to RNA-seq and metabolomic analysis to identify candidate genes and metabolites. The results indicated that genes and metabolites related to flavonoid biosynthesis and the MAPK signaling pathway may be involved in heat stress response. The results provide valuable information for the molecular breeding of resistant rose varieties.

Materials and methods

Plant materials and heat stress treatment

Two-year-old *Rosa hybrida* cv. "Francois Rabelais" rose cuttings (rootstock, *Rosa multiflora* Thunb.) were used as experimental materials. The plants were purchased from a nursery and pre-cultured in an artificial climatic chamber for 10 days under the following conditions: temperature of 24 °C, humidity of 55%, light duration of 12 h (day)/12 h (night), and light intensity of 100%. Subsequently, the artificial climatic chamber was set to 42 °C (persistent high-temperature weather in recent years in Hefei, Anhui Province, China) for 0 h (Treatment 0 h, T0), 3 h (T3), 6 h (T6), 9 h (T9), and 12 h (T12), respectively. After each treatment, functional leaves were collected, immediately frozen in liquid nitrogen, and stored in a −80 °C for subsequent transcriptome and metabolome sequencing. Transcriptome and metabolome analyses included three and six biological replicates, respectively.

Photosynthetic and antioxidant enzyme analyses

Plant leaves were collected to determine concentrations of photosynthetic pigments and proline. Samples (0.5 g fresh weight per treatment) were extracted in 80% (v/v) methanol and thoroughly ground. The concentration in the supernatant of this mixture was determined spectrophotometrically, as described by Wang and Huang [40]. Malondialdehyde (MDA), peroxidase (POD), and protein levels were analyzed using specific assay kits obtained from Nanjing Mo Fan Biotechnology Co., Ltd (Nanjing, China).

RNA extraction and sequencing

The total RNA of leaves was extracted according to the protocol for extraction of plant RNA (https://www.yuque.com/yangyulan-ayaeq/oupzan). After measuring the RNA levels and qualities, RNA was used to construct libraries according to the protocol for mRNA library preparation (BGI, China). The libraries were then sequenced using DNBSEQ (BGI, China). The SOAPnuke (v1.5.6) software was used for quality control of the raw data [41, 42]. The reference rose genome and annotation files were downloaded from the National Center for Biotechnology Information database (accession no. GCF_002994745.2) [43]. The clean data were mapped to the reference genome using HISAT (v2.1.0) [44]. Bowtie2 was applied to align the clean reads to the gene set, which included both known and novel transcripts as well as coding and noncoding transcripts [45]. Gene expression levels were calculated by RSEM (v1.3.1) [46]. Differentially expressed gene (DEG) analysis was performed using DESeq2 (v1.4.5) with a q-value ≤ 0.05 and $|\log_2(\text{Fold-change})| \geq 1$ [47]. Time series analysis was performed using Mfuzz (v2.34.0) [48], and gene coexpression network analysis was performed using WGCNA (v1.48).

Metabolite extraction and analysis

A total of 50 mg of tissues were extracted by directly adding 800 μL of precooled extraction reagent (MeOH: H_2O) (70:30, v/v, precooled at −20 °C); then, 20 μL of an internal standards mix was added for quality control of the sample preparation. Two small steel balls were added to the Eppendorf tube. After homogenization at 50 Hz for 5 min using TissueLyser (JXFSTPRP, China), samples were sonicated for 30 min at 4 °C and incubated at −20 °C for 1 h. The samples were then further centrifuged for 15 min at 14,000 rpm and 4 °C. Next, 600 μL of the supernatants were filtered through 0.22-μm microfilters and transferred to autosampler vials for liquid chromatography-mass spectrometry (LC-MS) analysis. To evaluate the reproducibility and stability of the whole LC-MS analysis, a quality control (QC) sample was prepared by pooling 20 μL of the supernatant from each sample.

Sample analysis was performed on a Waters ACQUITY UPLC 2D (Waters, USA) coupled to a Q-Exactive mass spectrometer (Thermo Fisher Scientific, USA) equipped with a heated electrospray ionization source. Chromatographic separation was performed on a Hypersil GOLD aQ column (2.1×100 mm, 1.9 μm, Thermo Fisher Scientific, USA) with mobile phase A consisting of 0.1% formic acid in water and mobile phase B consisting of 0.1% formic acid in acetonitrile. The column temperature was maintained at 40 °C. The gradient conditions were as follows: 5% B over 0.0–2.0 min, 5–95% B over 2.0–22.0 min, held constant at 95% B over 22.0–27.0 min, and washed with 95% B over 27.1–30 min. The flow rate was 0.3 mL/min, and the injection volume was 5 μL.

The mass spectrometric settings for the positive/negative ionization modes were as follows: spray voltage, 3.8/−3.2 kV; sheath gas flow rate, 40 arbitrary units (arb); aux gas flow rate, 10arb; aux gas heater temperature, 350 °C; and capillary temperature, 320 °C. The full scan range was 100–1,500 m/z with a resolution of 70,000, and the automatic gain control (AGC) target for MS acquisitions was set to 1e6, with a maximum ion injection time of 100 ms. The top three precursors were selected for subsequent mass spectrometry fragmentation with a maximum ion injection time of 50 ms and a resolution of 30,000; the AGC was 2e5. The stepped normalized collision energies were set to 20, 40, and 60 eV.

Metabolome data preprocessing

The raw data collected by LC-MS/MS were imported into Compound Discoverer 3.1 (Thermo Fisher Scientific, USA) for data processing. The molecular weight, retention time, peak area, and identification were derived from this analysis. Metabolites were identified using the BGI self-built standard library and the mzCloud database. Data preprocessing was performed using metaX [49]. The DAMs between groups were screened by multivariate statistical analysis using principal component analysis (PCA) and discriminant analysis, partial least squares method-discriminant analysis (PLS-DA) [50, 51], and univariate analysis using fold-change analysis and Student's t-test. DAM screening thresholds were as follows: variable importance in projection (VIP) values of the first two principal components of the PLS-DA model ≥ 1, Fold-Change ≥ 1.2 or ≤ 0.83, and q-value < 0.05.

Function enrichment analysis

Gene ontology (GO) (http://www.geneontology.org/) and Kyoto Encyclopedia of Genes and Genomes (KEGG) (https://www.kegg.jp/) enrichment analyses were performed using Phyper based on a hypergeometric test. Significant levels of terms and pathways were corrected using a q-value with a rigorous threshold (q-value ≤ 0.05).

Correlation analysis of RNA-seq and metabolomic data

The correlation between DEGs and DAMs was analyzed using regularized canonical correlation analysis (rCCA). Sparse partial least squares discriminant analysis (SPLSDA) was performed using the mixOmics package in R [52].

Quantitative real-time PCR

Total RNA was extracted and reverse transcribed into cDNA using the aforementioned method. Real-time qRT–PCR was performed using 20 μL of cDNA using the TB Green™ Premix Ex Taq™ II reagent (Takara; Tli RNaseH Plus); *Rc16S RNA* and *AtEF1a* were used as internal reference genes. The primers used for all detected genes are listed in Supplementary Table 1. Three biological replicates (each with three technical replicates) were subjected to the QuantStudio™ 6 Flex System (Applied Biosystems, USA) with the following amplification parameters: activation at 50 °C for 2 min, predenaturation at 95 °C for 2 min, denaturation at 95 °C for 15 s, and annealing at 60 °C for 1 min for 40 cycles. The relative gene expression levels were calculated using the $2^{-\Delta\Delta Ct}$ method.

RcHSP70 overexpression in arabidopsis and heat stress treatment

The *35 S::RcHSP70* vector was constructed and transformed into *A. tumefaciens* GV3101. Transformation of *Arabidopsis* ecotype Columbia-0 plants was performed using the floral dip method. For selection, seeds were planted under aseptic conditions on MS agar containing 25 mg L^{-1} hygromycin (primers see Supplementary Table 1). T3 lines displaying 100% hygromycin resistance were considered homozygous and used for further experiments [53]. Young seedlings were subjected to high-temperature conditions at 42 °C for 0 h, 0.5 h, 1 h, 2 h, and 3 h. *Arabidopsis* leaves overexpressing *RcHSP70* were collected to evaluate *RcHSP70* expression and heat response gene expression by qRT–PCR. The primers used are listed in Supplementary Table 1.

Results

Heat stress affects photosynthetic and antioxidant enzyme activities of *Rosa hybrdia*

The leaves *R. hybrida* did not exhibit significant wilting for a short period because of the presence of more wax but became softer because of water loss (Supplementary Fig. 1). The physiological function of *R. hybrida* is affected by heat stress. Analysis of physiological and biochemical indices at various periods after heat stress indicated chlorophyll and total protein content decreased significantly over time, reaching a minimum at 9 h before increasing/recovering (Fig. 1A-B). Similarly, the proline content increased significantly after heat stress, reaching a maximum at 9 h, and slightly decreased thereafter (Fig. 1C). Moreover, the POD activity level increased significantly and reached a maximum value at 6 h, followed by a rapid decrease (Fig. 1D). MDA content showed a similar trend to that of POD, but the increase was relatively weak (Fig. 1E).

RNA-sequencing and DEG screening

After the five groups of samples were sequenced and processed, clean reads were mapped to the rose genome, and the fragment per kilobase of transcript per million mapped value of each gene was calculated. PCA showed that the control group (T0) was significantly distinct from the treatment groups (T3, T6, T9, and T12), with some treatment groups being relatively close to each other, such as T3 and T9. The samples within each group could also be effectively clustered into multiple replicates, indicating high reproducibility (Fig. 2A). Since multiple treatment groups were not clustered with the control group, indicating that significant changes occurred in multiple treatment groups, comparing multiple treatment group time points with the control group showed 11,233 DEGs (5,855 upregulated and 5,378 downregulated genes) at

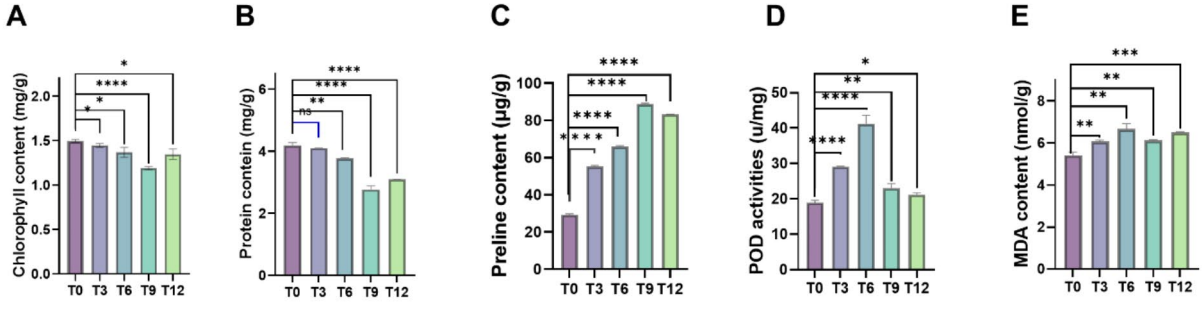

Fig. 1 Photosynthetic and antioxidant enzyme activities of *Rosa hybrida* after heat stress. (**A**) Total chlorophyll content. (**B**) Total protein content. (**C**) Proline content. (**D**)POD activities. (**E**) MDA content. Values are means ± SD ($n = 3$ biological replicates); Asterisks indicate statistically significant differences as determined by Student's *t*-test: ns, no significant; *, $P < 0.05$; **, $P < 0.01$; ***, $P < 0.001$; ****, $P < 0.0001$

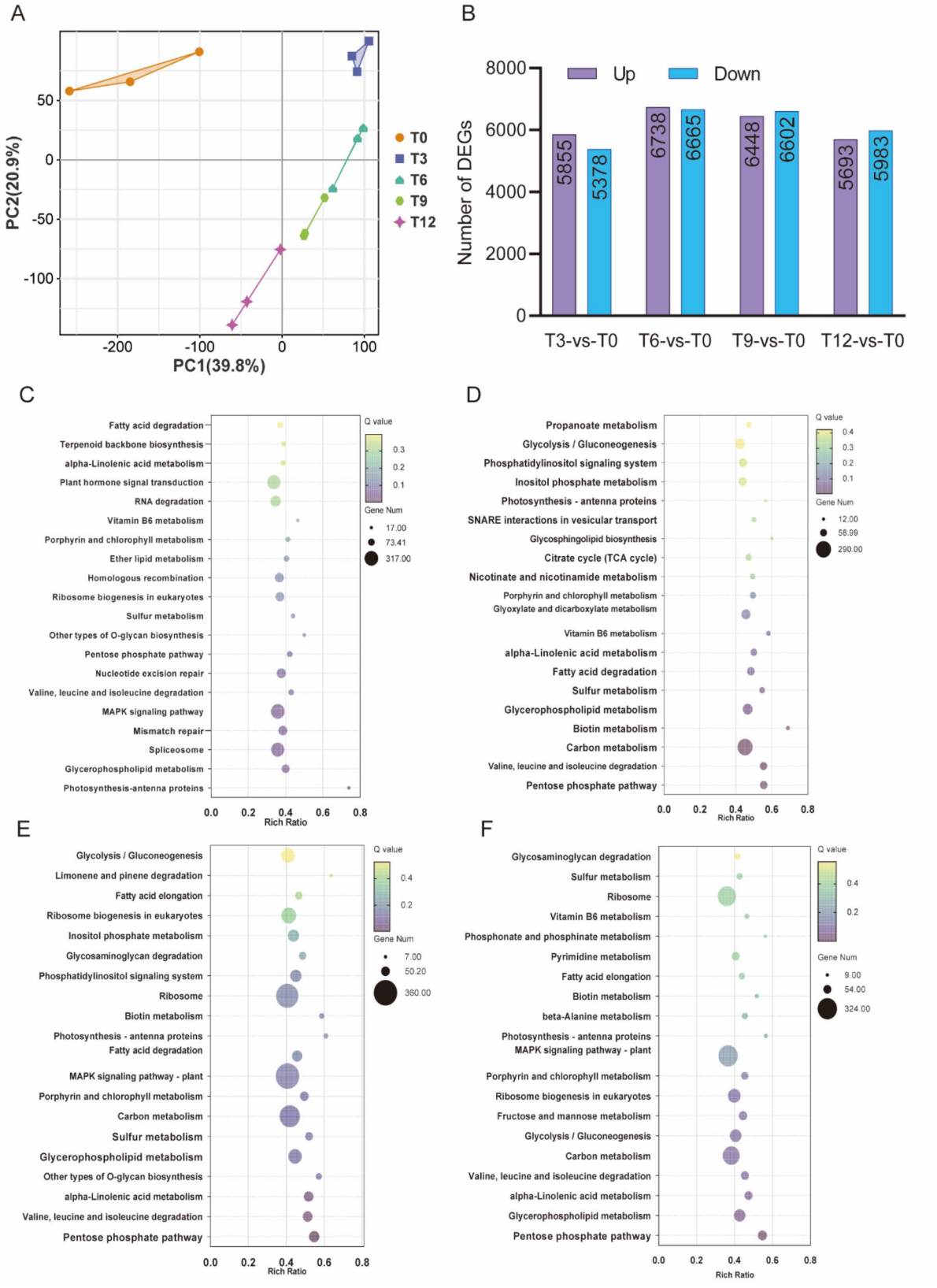

Fig. 2 Analysis of DEGs and the main KEGG pathways enriched by DEGs in *Rosa hybrida* response to heat stress. (**A**) PCA analysis of gene expression datasets. (**B**) Number of DEGs among compared groups. (**C**) KEGG analysis of DEGs between T0 and T3. (**D**) KEGG analysis of DEGs between T0 and T6. (**E**) KEGG analysis of DEGs between T0 and T9. (**F**) KEGG analysis of DEGs between T0 and T12. The color and size of the bubbles indicate significant enrichment and gene number, respectively

T3-vs-T0 and 13,403 DEGs at T6-vs-T0 (6,738 upregulated and 6,665down-regulated genes), T9-vs-T0 had 13,050 DEGs (6,448 upregulated and 6,602 downregulated genes), and T12-vs-T0 had 11,676 DEGs (5,693 upregulated and 5,983 downregulated genes; Fig. 2B).

Functional enrichment analysis of DEGs in the four compared groups showed that the common enriched pathways included alpha-linolenic acid metabolism, sulfur metabolism, pentose phosphate pathway, glycerophospholipid metabolism, porphyrin metabolism, and chlorophyll metabolism, etc. (Fig. 2C–F). In addition, some pathways were enriched only in the T3-vs-T0 comparison group, such as homologous recombination, nucleotide excision repair, terpenoid backbone biosynthesis, RNA degradation, spliceosomes, plant hormone signal transduction, and ether lipid metabolism (Fig. 2C); and the glyoxylate and dicarboxylate metabolism, glycosphingolipid biosynthesis, propanoate metabolism, nicotinate and nicotinamide metabolism, citrate cycle, and SNARE interactions in vesicular transport pathways were enriched only in the T6-vs-T0 comparison group (Fig. 2D). Further, limonene and pinene degradation was only enriched in the T9-vs-T0 comparison group (Fig. 2E), and fructose and mannose metabolism, phosphonate and phosphinate metabolism, beta-amylase metabolism, alanine metabolism, beta-amylase metabolism, and pyrimidine metabolism were only enriched in the T12-vs-T0 group (Fig. 2F).

Function enrichment of DEGs in response to heat stress

Further analysis of the four comparison group identified 4,652 common DEGs (Fig. 3A); the corresponding enriched metabolic pathways were plant–pathogen interaction, MAPK signaling pathway, spliceosome, mismatch repair, pentose phosphate pathway, homologous recombination, DNA replication, etc. (Fig. 3B). According to the pattern of gene expression changes during heat stress, the expression of genes in cluster 6 gradually increased after heat stress treatment, reaching a peak at 6–9 h. The expression of genes in cluster 8 gradually decreased after heat stress treatment, reaching the lowest point at 6–12 h (Fig. 3C, Supplementary Tables 2 and 3). The genes in clusters 6 and 8 were mostly consistent with trends in changes detected in physiological indices and antioxidant activities. Functional analysis of the genes in cluster 6 showed that they were mainly related to spliceosome (such as classic heat-responsive proteins, HSP70 homology genes: LOC112182696, LOC112173817, and BGI_novel_G003858), mismatch repair, DNA replication, sulfur metabolism, etc. (Fig. 3D, Supplementary Table 2). Significantly enriched cluster 8 genes included plant–pathogen interaction, phenylpropanoid biosynthesis, flavonoid biosynthesis, MAPK signaling pathway, etc. (Fig. 3E).

Metabolomic changes in *R. hybrida* in response to heat stress

Further metabolomic examination of the heat-treated samples showed high reproducibility of both positive-ion mode (pos) metabolites and negative-ion mode (neg) metabolites in samples from multiple time points (Fig. 4A-B, Supplementary Table 4). A total of 723 pos metabolites and 432 neg metabolites were identified (Fig. 4C), mainly containing flavonoids (60 positive metabolites and 52 negative metabolites), terpenoids (39 positive metabolites and 33 negative metabolites), phenylpropanol (33 positive metabolites and 23 negative metabolites), phenols (15 positive metabolites and 15 negative metabolites), phenolic acids (16 positive metabolites and 11 negative metabolites), and others (Fig. 4D). Comparison of DAMs between the four treatment groups and the control group showed 243 DAMs (including 144 positive and 89 negative metabolites) in the T3-vs-T0 comparison group, 254 DAMs (including 157 positive and 97 negative) in the T6-vs-T0 comparison group, 246 DAMs in the T9-vs-T0 comparison group (including 165 positives and 81 negatives), and 265 DAMs in the T12-vs-T0 comparison group (including 174 positives and 91 negatives; Fig. 4E).

Enrichment analysis of the DAMs in the four comparison groups showed that the enriched pos DAMs in KEGG metabolic pathways included alpha-linolenic acid metabolism and arginine biosynthesis, whereas the neg DAMs were enriched in pathways such as plant hormone signal transduction, cyano amino acid metabolism, tropane, piperidine and pyridine alkaloid biosynthesis, aminoacyl-tRNA biosynthesis, phenylpropanoid biosynthesis, and glucosinolate biosynthesis (Fig. 4F–I). In addition, pos DAMs were significantly enriched in ABC transporters in the T6/9/12-vs-T0 comparison group, except at the early stage of heat stress treatment (T3-vs-T0), which is related to the transmembrane transport of metabolites at the later stage of the treatment (Fig. 4F–I).

DAMs in response to heat stress

Further analysis identified 57 common DAMs in the four comparison groups (Fig. 5A). These 57 DAMs were significantly enriched in the pathway of aminoacyl-tRNA biosynthesis, glucosinolate biosynthesis, and cyano amino acid metabolism and were associated with two major metabolites, L-isoleucine and L-phenylalanine (Fig. 5B). Analysis of the changes in the content of these DAMs revealed three clusters, cluster I showed the lowest content at T0, which increased significantly from T3 to T12; the changes in these metabolites were consistent with the trend in the changes in POD activity, proline, and MDA content. In cluster III, the trend was almost the opposite, with the highest content at T0, decreasing significantly thereafter; the trend was also consistent

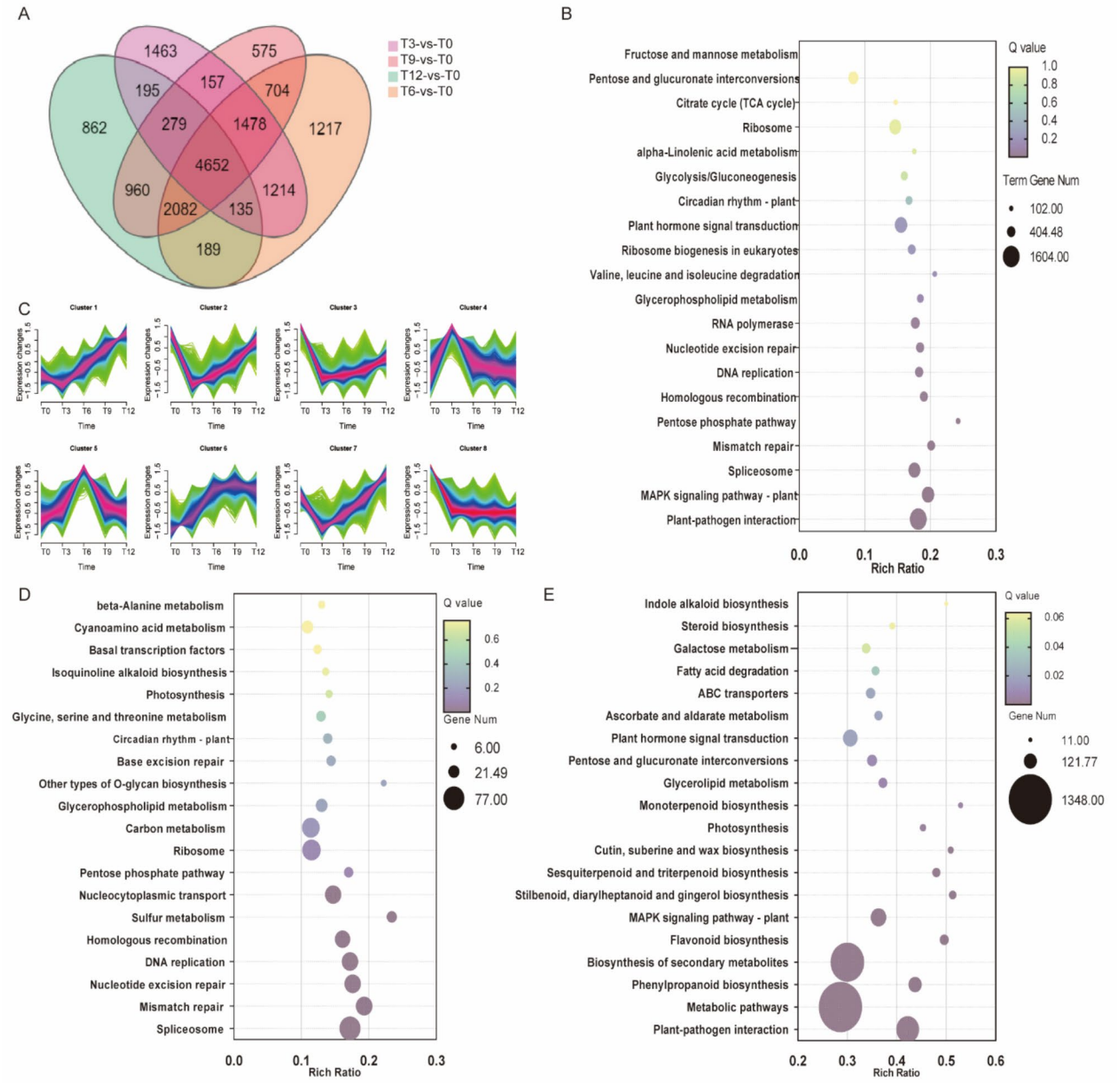

Fig. 3 Venn diagram of the comparison groups and function enrichment analysis. (**A**) Venn diagram of the four comparison groups. (**B**) KEGG analysis of common DEGs in four comparison groups. (**C**) The trend pattern analysis of all genes expression level. (**D**) KEGG analysis of cluster 6 genes in Fig. 3C. (**E**) KEGG analysis of cluster 8 genes in Fig. 3C. The color and size of the bubbles indicate significant enrichment and gene number, respectively

with the trend of changes in chlorophyll and total protein content. In addition, the content of cluster I; metabolites decreased at T3, followed by a rapid increase at T6 and a subsequent rapid decrease (Fig. 5C).

Combined RNA-seq and metabolomic analysis

The Spearman correlation coefficient was calculated for DEGs and DAMs. Network diagrams were plotted for DEGs and DAMs with absolute correlation coefficient values > 0.9 and p-value < 0.05 (Fig. 6A). The significant nodes in the four comparison groups were L-phenylalanine, jasmonic acid, 5-fluoro, and biocytin, which may play key roles in the plant's response to heat stress (Fig. 6B–E). The patterns of content changes divided the metabolites into three subgroups: cluster 1, upregulated after heat shock (T3–T12); cluster 2, downregulated after heat shock (T3–T12); cluster 3, increased at T6 and later decreased (Fig. 6F). This trend was consistent with the results shown in Fig. 5C. In addition, the DAMs and DEGs in the four comparison groups were mainly enriched in alpha-linolenic acid metabolism,

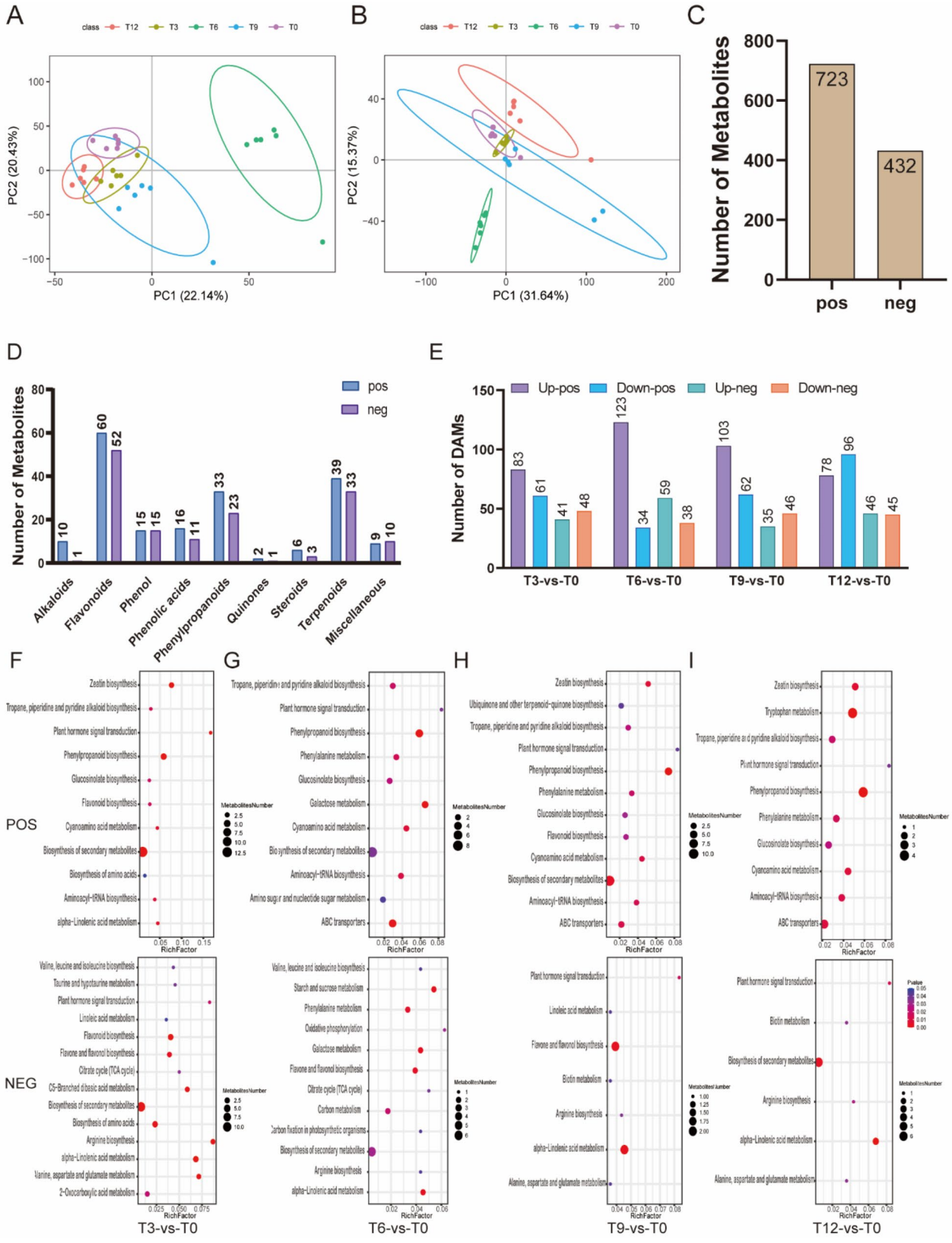

Fig. 4 DAMs of *Rosa hybrida* in response to heat stress. (**A**) Principal component analysis of pos metabolites. (**B**) Principal component analysis of neg metabolites. (**C**) Number of identify metabolites. (**D**) Classified of metabolites. (**E**) Number of DAMs among compared groups. (**F**) KEGG analysis of DAMs between T3-vs-T0. (**G**) KEGG analysis of DAMs between T6-vs-T0. (**H**) KEGG analysis of DAMs between T9-vs-T0. (**I**) KEGG analysis of DAMs between T12-vs-T0

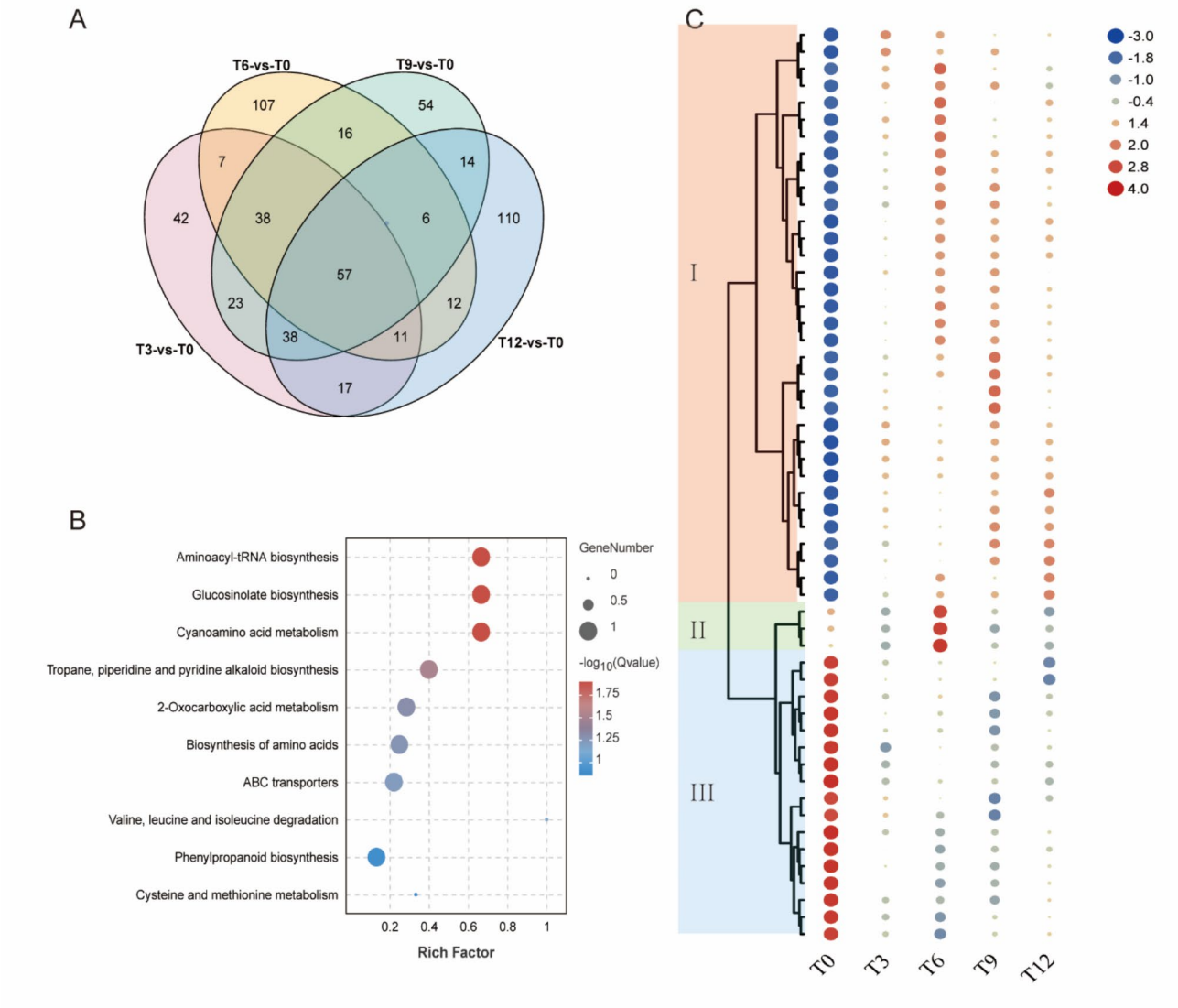

Fig. 5 Venn diagram of DAMs in the comparison groups and function enrichment analysis. (**A**) Venn diagram of DAMs in the four comparison groups. (**B**) KEGG analysis of common DAMs in four comparison groups. (**C**) The heatmap of common DAMs in the four comparison groups. Three subgroups marked with cluster I, II, III

plant hormone signal transduction, and phenylpropanoid biosynthesis (Fig. 6G).

Heat stress response pathways

After heat stress, phenylpropanoid and downstream flavonoid biosynthesis were enriched in roses. Multiple hormones are involved in the regulation of the heat stress process. In the flavonoid biosynthesis pathway, the expression levels of *CHI*, *HCT* (excluding 112197593 and 112165685), *FLS*, and *DFR* were downregulated after heat stress. Four metabolites in this pathway showed significant changes, pinocembrin and dihydroquercetin levels decreased after heat treatment, and eriodictyol and dihydromyricetin levels increased trend after heat stress (Fig. 7A).

The significant enrichment of plant hormone signal transduction and MAPK signaling indicates a close relationship between these two pathways. We analyzed jasmonic acid and ethylene-related pathways in the MAPK signaling pathway. The expression levels of *MKK3* and *MPK6* were significantly downregulated after heat stress, which acts as an inhibitor of *MYC2* and causes upregulation of *MYC2* homology (except 112200522). In addition, *ERF1* repression (whose expression levels increased after heat stress) plays a role in the regulation of *VSP2* expression (Fig. 7B). In the ethylene signaling pathway, *RAN1*,

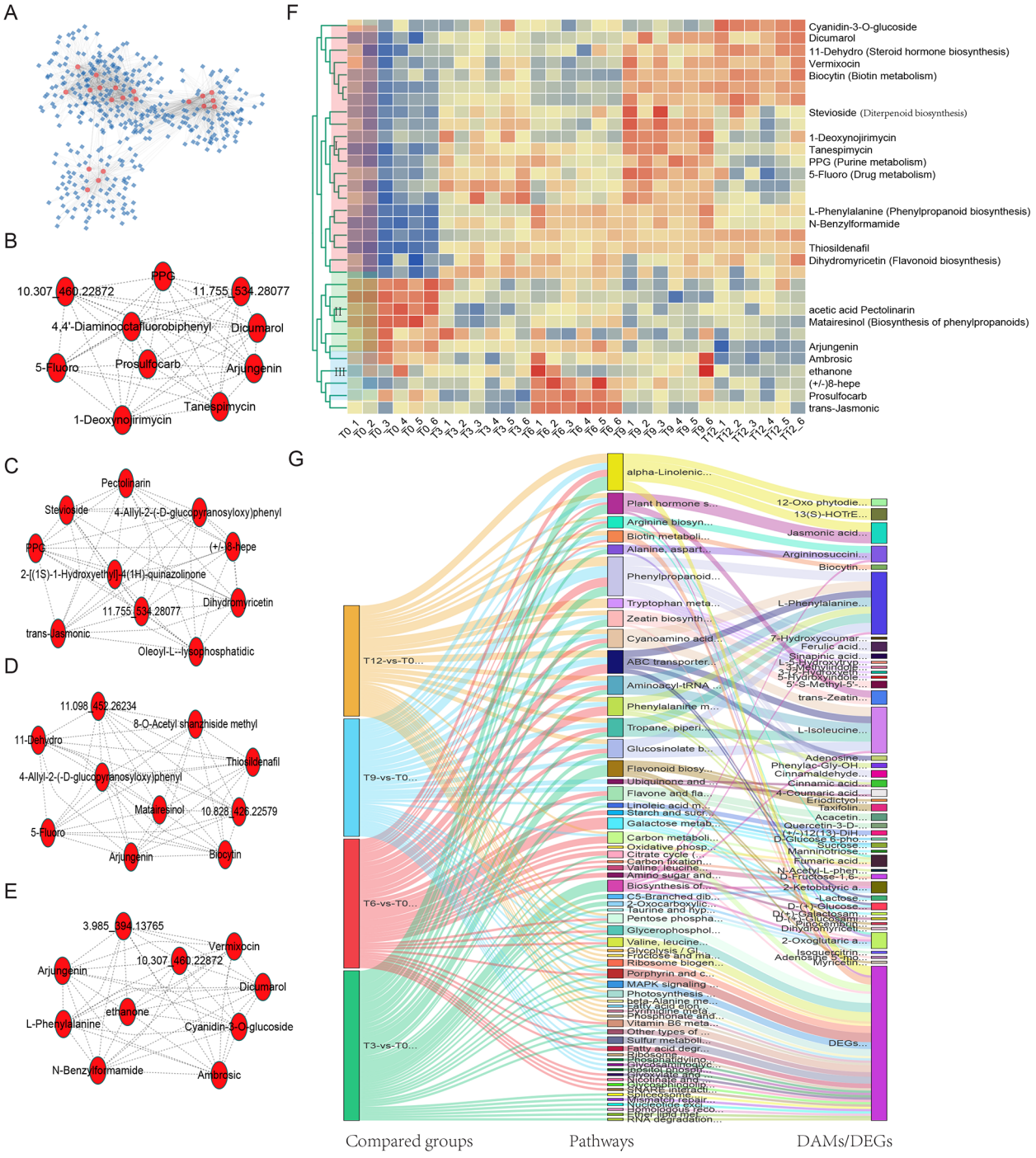

Fig. 6 The connection network between DEGs and DAMs. (**A**)The schematic of network between DEGs and DAMs. The rhomboid and dots represent genes and metabolites, respectively. (**B**) The top10 core nodes DAMs in compared group T3-vs-T0. (**C**) The top10 core nodes DAMs in compared group T6-vs-T0. (**D**) The top10 core nodes DAMs in compared group T9-vs-T0. (**E**) The top10 core nodes DAMs in compared group T12-vs-T0. (**F**) The heatmap of core DAMs in four compared groups. Log_2-scaled metabolites content are shown, ranging from low (blue) to high (red). Three subgroups marked with cluster I, II, III. (**G**) Sankey diagram showing the relationship between pathways and DAMs/DEGs, the DEGs number were more than 4000, the gene names were not showed

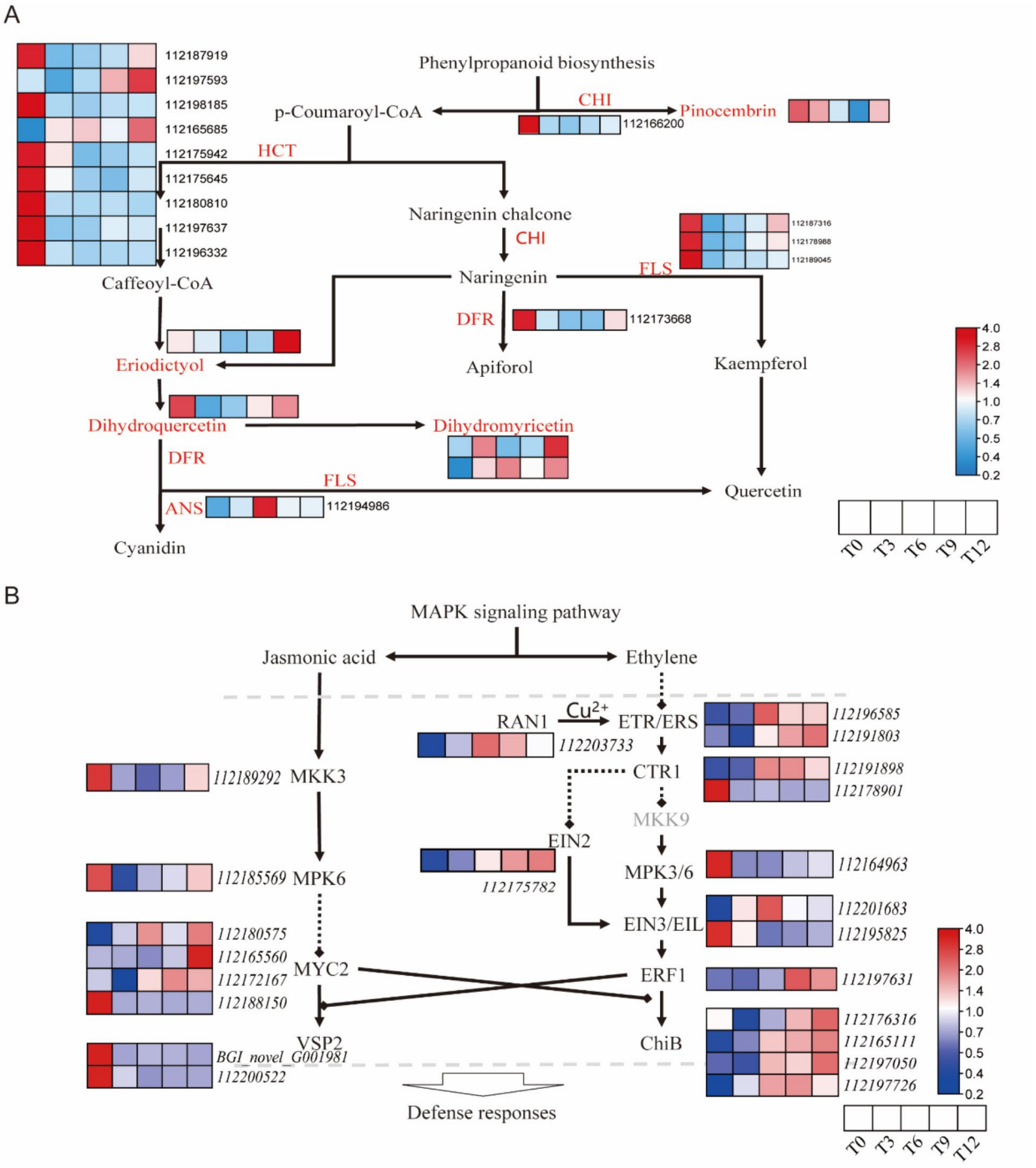

Fig. 7 The pathways of flavonoid biosynthesis and MAPK signaling pathway response to heat stress. (**A**) The flavonoid biosynthesis pathways. HCT: shikimate O-hydroxycinnamoyltransferase; FLS: flavonol synthase; DFR: bifunctional dihydroflavonol 4-reductase/flavanone 4-reductase; ANS: anthocyanidin synthase; CHI: chalcone isomerase. (**B**) The MAPK signaling pathway. MKK3: mitogen-activated protein kinase kinase 3; MPK6: mitogen-activated protein kinase 6; MYC2: transcription factor MYC2; VSP2: vegetative storage protein 2; RAN1/copA, P-type Cu + transporter; ETR/ERS: ethylene receptor; CTR1: serine/threonine-protein kinase; MPK3: mitogen-activated protein kinase 3; MPK6: mitogen-activated protein kinase 6; EIN2/3: ethylene-insensitive protein 2/3; ERF1: ethylene-responsive transcription factor 1; ChiB: basic endochitinase B. Log2-scaled FPKM or metabolites content are shown in different time points of leaf (here T0-T12, from left to right in each heatmap panel) are presented in the heatmap alongside the gene id. Low to high expression is indicated by a change in color from blue to red

ETR, and *CTR1* (excluding 112178901) significantly increased their expression levels while *MPK3/6* expression was inhibited. In addition, *MYC2*, which is involved in the ethylene pathway and coordinates the regulation of *ChiB* expression levels, upregulated the expression of a homologous ChiB protein after heat stress (Fig. 7B).

RNA-seq expression validation by qRT–PCR

qRT–PCR was used to confirm the reliability of our RNA-seq data. The results revealed that the expression patterns of 16 selected DEGs were consistent with the RNA-seq data sets (Fig. 8). Among these genes, *HSP70*, a typical maker gene in response to heat stress, was significantly upregulated after heat stress. RBOP, PR1, and four WRKY transcript factors, crucial genes in the MAPK signaling pathway, were downregulated after heat stress, suggesting that heat stress regulates resistance to high temperatures (Fig. 8).

RcHSP70 overexpression decreases *Arabidopsis*'s timely responses to high temperatures

To determine whether *RcHSP70* confers resistance to heat stress, *RcHSP70* was introduced into *Arabidopsis* wild-type (WT). After high-temperature treatment, *RcHSP7* OE plants showed higher resistance to high temperature, but WT plants showed an earlier wilting phenotype (Fig. 9A). High *RcHSP70* expression was also detected in *Arabidopsis* OE plants using qRT–PCR (Fig. 9B). The expression levels of four known heat-responsive genes in *Arabidopsis* were examined, and the results revealed that the expression of Hsp70-interacting protein genes (*HIP*) was significantly increased in OE2 plants compared with WT plants at 1 h after high-temperature treatment. At 0.5 h after high temperature, expression of the 9-cis-epoxy carotenoid dioxygenase gene (*NCED*) was significantly decreased compared with that in WT plants. The trends of phytochrome interacting factor 4 (*PIF*) and ascorbate peroxidase 6 (*APX*) expression were essentially the same in WT and OE2 (Fig. 9C).

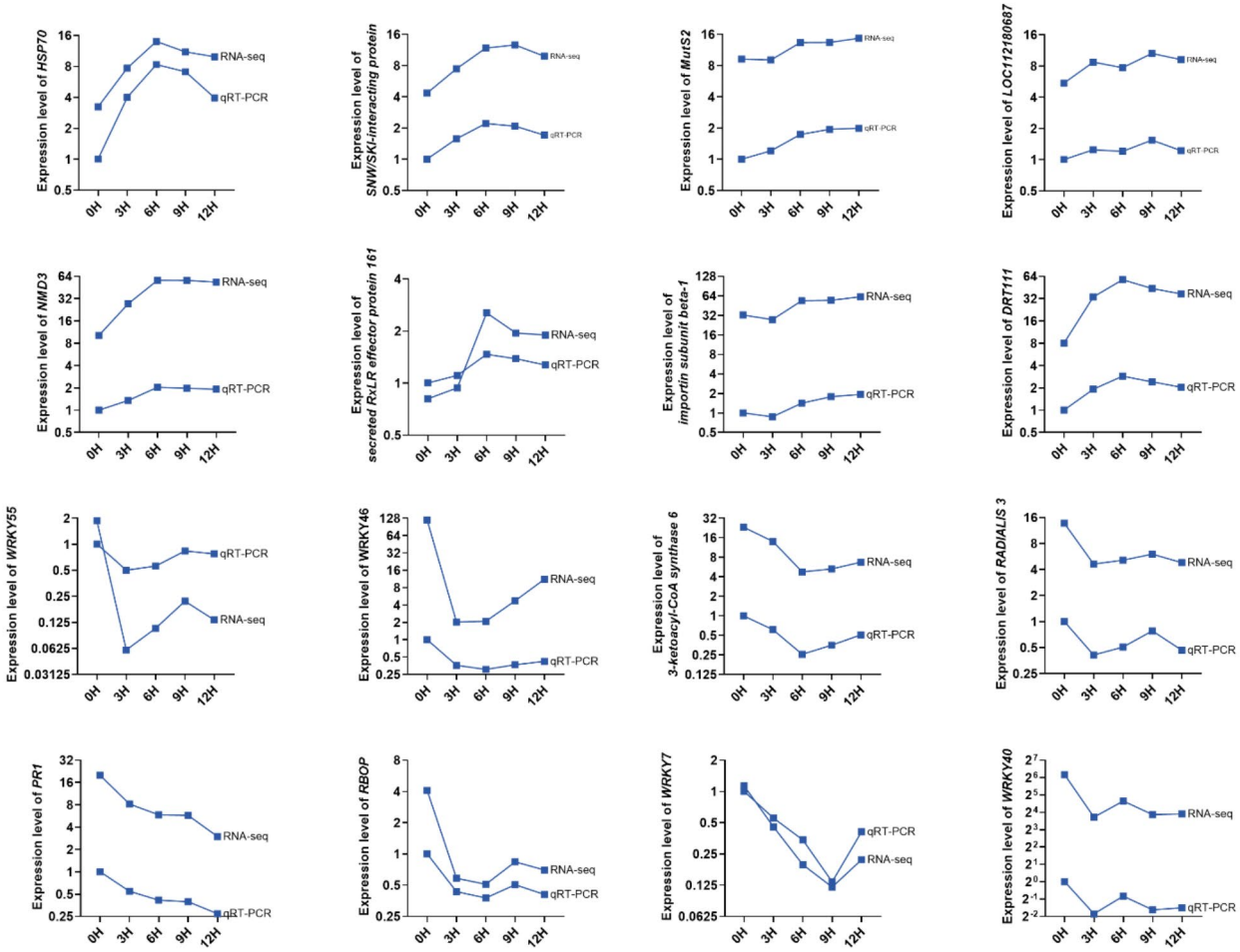

Fig. 8 Expression pattern of the selected 16 genes

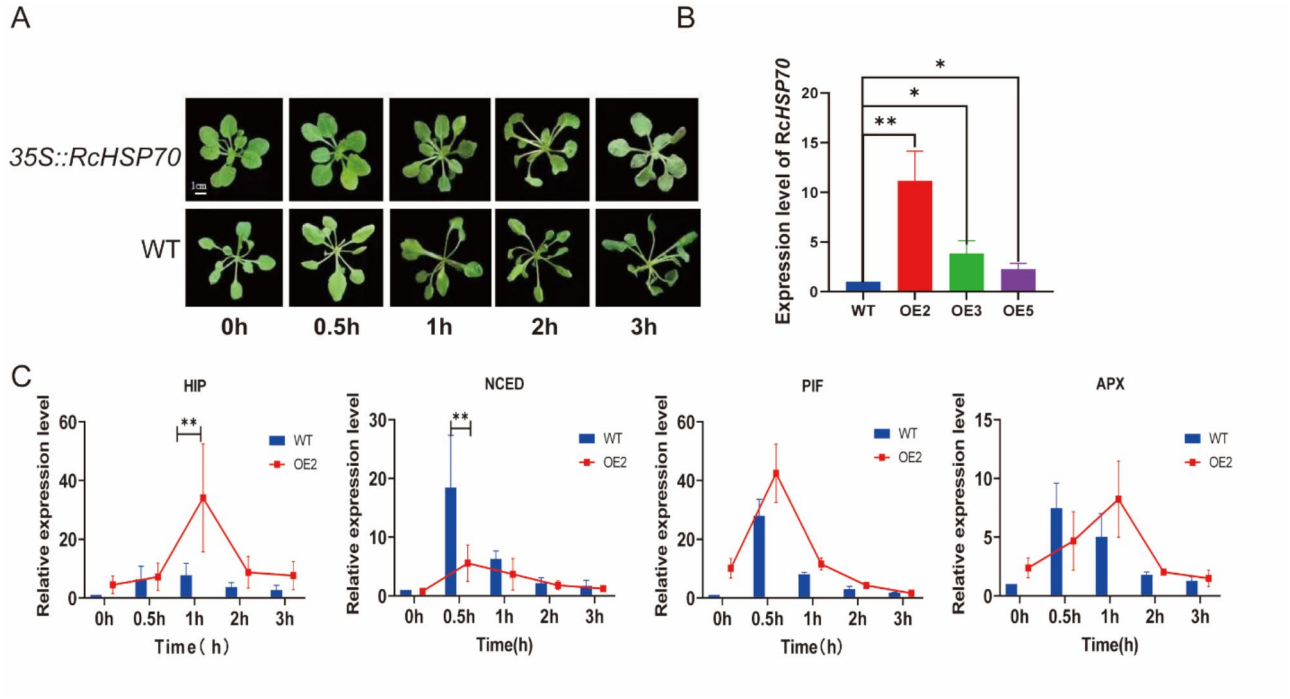

Fig. 9 The *RcHSP70* gene enhance the resistance of *Arabidopsis* to heat stress. (**A**) Representative images showed the resistance of *Arabidopsis* to heat stress. (**B**) qRT-PCR analysis of *RcHSP70* expression in WT, OE2, OE3, and OE5 lines. 16 S was used as the reference gene. (**C**) qRT-PCR analysis of five heat response genes in WT and OE2. PIF, phytochrome interacting factor 4; HIP, Hsp70-interacting protein; NCED, 9-cis-epoxycarotenoid dioxygenase; APX, ascorbate peroxidase 6. Values are means ± SD of three technical replicates. *, $P < 0.05$; **, $P < 0.01$

Discussion

As an important ornamental plant, roses hold a high market share in the flower industry and have significant economic value. Breeding varieties that are resistant to high temperatures is crucial for increasing the production of rose flowers. Although key genes involved in heat stress responses have been reported in other species, whether the regulatory and responsive mechanisms of roses are consistent with those of these species remains unclear. Li et al. conducted a preliminary exploration of heat stress-responsive genes in roses via transcriptome analysis, but there is still a lack of systematic research on the relationship between gene and metabolite changes after heat stress [4]. This study further explored the characteristics of gene and metabolite changes in roses induced by high temperatures using transcriptomic and metabolomic methods.

In this study, we found a higher number of DEGs at T6 and T9 than at T3 and T12, indicating the impact of heat stress on the rose peaks at T6 and T9. This finding was generally consistent with multiple physiological indicators, such as the lowest chlorophyll and protein content at T9 and the highest proline content at T9. POD and MDA activities reached peaked at T6. Typically, plant activity is inhibited under high-temperature stress, leading to suppressed protein and chlorophyll synthesis. Both substances reached their lowest levels around 9 h after heat stress, suggesting that the impact of heat stress on roses may be less severe during the early stages or within 9 h of continuous heat stress. The accumulation of proline helps plants tolerate high-temperature stress [54–56]. In roses, the proline content peaked after 9 h of high-temperature stress. POD and MDA activity is usually associated with a plant's ability to cope with stress, indicating that roses gradually accumulate substances to resist high temperatures during stress responses.

In this study, the enrichment of DEGs and DAMs exhibited high similarity. Significant enrichments were observed in pathways such as alpha-linolenic acid metabolism, flavonoid biosynthesis, phenylpropanoid biosynthesis, plant hormone signal transduction, and the MAPK signaling pathway, suggesting a strong correlation between DEGs and DAMs. As reported, flavonoids have a short-term effect on heat stress in *Anoectochilus roxburghii* [57], and flavonoid accumulation regulation through hormones reduces heat stress in rice [58]. In this study, the expression of multiple genes during flavonoid biosynthesis exhibited a decreasing trend. Similarly, the contents of several metabolites (eriodictyol, dihydroquercetin, and pinocembrin) in this pathway decreased during the early stages of heat stress, consistent with gene expression trends. Flavonoids have strong antioxidant activity and can reduce the damage caused by heat stress [59–61], which may be beneficial for enhancing

heat tolerance in roses by increasing the expression of genes in the flavonoid biosynthesis pathway and thus the metabolite content of the pathway.

In addition, plant hormones and MAPK signaling are involved in various stress responses [62–66]. The MAPK pathway responds to pathogen infection and plays a crucial role in the regulation of plant hormones, cold, salt, drought, and wounding [65, 66]. In this study, plant hormones and MAPK signaling were significantly enriched after high-temperature stress, indicating that heat stress may share common pathways with multiple abiotic stresses. In particular, regulatory pathways involving jasmonic acid and ethylene exhibited different expression patterns. Multiple genes in the jasmonic acid pathway tended to decrease in expression after high-temperature stress, whereas genes in the ethylene pathway did the opposite. Although both pathways are involved in defense responses, further research is needed to determine whether gene expression changes are due to heat stress induction or resistance responses. Jasmonic acid accumulation improves heat tolerance in plants, and increased ethylene content tends to promote plant senescence [67–69]. The results of this study revealed that increasing the expression of genes in the jasmonic acid pathway, such as *MKK3*, *MPK6*, and *VSP2*, and decreasing the expression of *RAN1*, *ETR*, and *ChiB* in the ethylene pathway may be beneficial for improving heat tolerance in roses. In addition, pos DAMs were significantly enriched in ABC transporters, which are mainly involved in the transport of some metabolites. Although the ABC transporter Pdr18 was found to be required for thermotolerance in yeast [70], whether ABC transporters are involved in thermotolerance in plant need further research.

HSP70s are crucial response proteins and markers for detecting heat stress in plants [6, 71, 72]. HSP70s are diverse and possess the important function of restoring proteins denatured due to heat stress to their undenatured states [7]. Therefore, the high expression and constitutive presence of HSP70s in plants imparts potential for the timely restoration of denatured proteins. HSP70s participate in heat stress response processes in a variety of plant species, such as *Arabidopsis*, rice, and jujube [73–77]. An *RcHSP70* homolog has been cloned into heat-tolerant Chinese rose varieties [78]. In *R. hybrida*, HSP70s are a large family that may cause differences in the responses to heat tolerance in different varieties. In this study, we heterologously overexpressed a selected HSP70 protein from the "Francois Rabelais" rose variety of *Arabidopsis thaliana*, and the results confirmed that overexpression of RcHSP70 confers a significant advantage to *Arabidopsis* plants in terms of resisting high-temperature stress. In addition, HIP cooperates with HSP70 to facilitate protein folding and prevent aggregation [79]. The expression level of HIP was significantly increased in OE2 *Arabidopsis* plants, suggesting that HIP interact with RcHSP70. *NCED* was positively regulated in rice and *Arabidopsis* under heat and drought stress [80, 81]. However, *NCED* expression was significantly lower in OE2 *Arabidopsis* than in WT plants after 0.5 h of heat stress treatment. The expression levels of *PIF* and *APX* were upregulated after heat stress treatment, but there was no significant difference between WT and OE2 *Arabidopsis* plants [82, 83]. These results suggest that RcHSP70 contributes to the response to high-temperature stress and participates in high-temperature tolerance in *Arabidopsis.*

Conclusions

This study examined genetic and biochemical changes in rose plants at five time points after heat stress. Based on transcriptomic and metabolomic analyses in four comparison groups, we identified 4,652 potential DEGs and 57 DAMs. These DEGs and DAMs were found to be enriched in several pathways, including phenylpropanoid biosynthesis, MAPK signaling, and alpha-linolenic acid metabolism. Flavonoids and plant hormones play crucial roles in enhancing the resistance of rose plants to heat stress. In addition, *RcHSP70* decreased the timely response to high temperatures in *Arabidopsis*. Our findings provide insights into the response of rose plants to high temperatures and can serve as a foundation to improve their resistance to heat stress.

Abbreviations

MDA	Malondialdehyde
POD	Peroxidase
DEG	Differentially expressed gene
DAMs	Differentially abundant metabolites
MAPK	Mitogen-activated protein kinases
HSP	Heat shock proteins
ROS	Reactive oxygen species
HfA1	Heat shock transcription factor A1
LC	MS-Liquid chromatography mass spectrometry
QC	Quality control
AGC	Automatic gain control
PCA	Principal component analysis
PLS	DA-Partial least squares method-discriminant analysis
VIP	Variable importance in projection
GO	Gene ontology
KEGG	Kyoto Encyclopedia of Genes and Genomes
rCCA	Regularized Canonical correlation analysis
SPLSDA	Sparse partial least squares discriminant analysis
pos	Positive ion mode
neg	Negative ion mode
PIF	Phytochrome interacting factor 4
HIP	Hsp70-interacting protein
NCED	9-Cis-epoxycarotenoid dioxygenase
APX	Ascorbate peroxidase 6; WT, wild-type
OE	Overexpression
HCT	Shikimate O-hydroxycinnamoyl transferase
FLS	Flavonol synthase
DFR	Bifunctional dihydroflavonol 4-reductase/flavanone 4-reductase
ANS	Anthocyanidin synthase
CHI	Chalcone isomerase
MKK3	Mitogen-activated protein kinase kinase 3

MPK6	Mitogen-activated protein kinase 6
MYC2	Transcription factor MYC2
VSP2	Vegetative storage protein 2
RAN1/copA	P-type Cu + transporter
ETR/ERS	Ethylene receptor
CTR1	Serine/threonine-protein kinase
MPK3	Mitogen-activated protein kinase 3
MPK6	Mitogen-activated protein kinase 6
EIN2/3	Ethylene-insensitive protein 2/3
ERF1	Ethylene-responsive transcription factor 1
ChiB	Basic endochitinase B

Supplementary Information

The online version contains supplementary material available at https://doi.org/10.1186/s12870-024-05543-1.

Supplementary Material 1: Supplementary Figure 1. *R. hybrida* were treated with heat stress

Supplementary Material 2

Supplementary Material 3

Supplementary Material 4

Supplementary Material 5

Supplementary Material 6

Acknowledgements
Not applicable.

Author contributions
H.W. conceived the study; W.X., X.Z. and S.Z. analyzed the data; S.Z. was involved in data interpretation; R.L. and A.R. prepared figures and tables; S.J. and W.L. collected the samples and performed the experiments; H.W. and L.W. wrote the article. All authors read and approved the final version of the manuscript.

Funding
This work was supported by the key research and development project in Anhui Province (202104a06020017).

Data availability
All the RNA-seq raw data used in this study have been deposited at NCBI BioProject under accession number PRJNA1090540 and are available at the following http://www.ncbi.nlm.nih.gov/bioproject/1090540. All the metabolomics data supporting the findings of this study are available within the paper and its Supplementary Information files. Should any raw data files be needed in another format they are available from the corresponding author upon reasonable request.

Declarations

Ethics approval and consent to participate
The use of plant parts in the present study complies with international, national and/or institutional guidelines.

Consent for publication
Not applicable.

Competing interests
The authors declare no competing interests.

Author details
[1]School of Horticulture, Anhui Agricultural University, Hefei 230036, China
[2]Horticulture Branch, Heilongjiang Academy of Agricultural Sciences, Harbin 150069, China

Received: 19 April 2024 / Accepted: 23 August 2024
Published online: 20 September 2024

References

1. Lesk C, Rowhani P, Ramankutty N. Influence of extreme weather disasters on global crop production. Nature. 2016;529(7584):84–7.
2. Hasanuzzaman M, Nahar K, Alam MM, Roychowdhury R, Fujita M. Physiological, biochemical, and molecular mechanisms of heat stress tolerance in plants. Int J Mol Sci. 2013;14(5):9643–84.
3. Jiang C, Xu J, Zhang H, Zhang X, Shi J, Li M, Ming F. A cytosolic class I small heat shock protein, RcHSP17.8, of Rosa chinensis confers resistance to a variety of stresses to Escherichia coli, yeast and Arabidopsis thaliana. Plant Cell Environ. 2009;32(8):1046–59.
4. Li ZQ, Xing W, Luo P, Zhang FJ, Jin XL, Zhang MH. Comparative transcriptome analysis of Rosa chinensis 'Slater's crimson China' provides insights into the crucial factors and signaling pathways in heat stress response. Plant Physiol Biochem. 2019;142:312–31.
5. Morimoto RI. The heat shock response: systems biology of proteotoxic stress in aging and disease. Cold Spring Harb Symp Quant Biol. 2012;76(0):91–9.
6. Kotak S, Larkindale J, Lee U, von Koskull-Döring P, Vierling E, Scharf KD. Complexity of the heat stress response in plants. Curr Opin Plant Biol. 2007;10(3):310–6.
7. Qu AL, Ding YF, Jiang Q, Zhu C. Molecular mechanisms of the plant heat stress response. Biochem Biophys Res Commun. 2013;432(2):203–7.
8. Suzuki N, Mittler R. Reactive oxygen species and temperature stresses: a delicate balance between signaling and destruction. Physiol Plant. 2006;126(1):45–51.
9. Baxter A, Mittler R, Suzuki N. ROS as key players in plant stress signalling. J Exp Bot. 2013;65(5):1229–40.
10. Mishra SK, Tripp J, Winkelhaus S, Tschiersch B, Theres K, Nover L, Scharf KD. In the complex family of heat stress transcription factors, HsfA1 has a unique role as master regulator of thermotolerance in tomato. Genes Dev. 2002;16(12):1555–67.
11. Yoshida T, Ohama N, Nakajima J, Kidokoro S, Mizoi J, Nakashima K, Maruyama K, Kim JM, Seki M, Todaka D, et al. Arabidopsis HsfA1 transcription factors function as the main positive regulators in heat shock-responsive gene expression. Mol Genet Genomics: MGG. 2011;286(5–6):321–32.
12. Sato H, Mizoi J, Tanaka H, Maruyama K, Qin F, Osakabe Y, Morimoto K, Ohori T, Kusakabe K, Nagata M, et al. Arabidopsis DPB3-1, a DREB2A interactor, specifically enhances heat stress-induced gene expression by forming a heat stress-specific transcriptional complex with NF-Y subunits. Plant Cell. 2014;26(12):4954–73.
13. Liu J, Sun N, Liu M, Liu J, Du B, Wang X, Qi X. An autoregulatory loop controlling Arabidopsis HsfA2 expression: role of heat shock-induced alternative splicing. Plant Physiol. 2013;162(1):512–21.
14. Bharti K, Von Koskull-Döring P, Bharti S, Kumar P, Tintschl-Körbitzer A, Treuter E, Nover L. Tomato heat stress transcription factor HsfB1 represents a novel type of general transcription coactivator with a histone-like motif interacting with the plant CREB binding protein ortholog HAC1. Plant Cell. 2004;16(6):1521–35.
15. Guan Q, Yue X, Zeng H, Zhu J. The protein phosphatase RCF2 and its interacting partner NAC019 are critical for heat stress-responsive gene regulation and thermotolerance in Arabidopsis. Plant Cell. 2014;26(1):438–53.
16. Liu HT, Li GL, Chang H, Sun DY, Zhou RG, Li B. Calmodulin-binding protein phosphatase PP7 is involved in thermotolerance in Arabidopsis. Plant Cell Environ. 2007;30(2):156–64.
17. Qin F, Sakuma Y, Tran LS, Maruyama K, Kidokoro S, Fujita Y, Fujita M, Umezawa T, Sawano Y, Miyazono K, et al. Arabidopsis DREB2A-interacting proteins function as RING E3 ligases and negatively regulate plant drought stress-responsive gene expression. Plant Cell. 2008;20(6):1693–707.
18. Yoo CY, Miura K, Jin JB, Lee J, Park HC, Salt DE, Yun DJ, Bressan RA, Hasegawa PM. SIZ1 small ubiquitin-like modifier E3 ligase facilitates basal thermotolerance in Arabidopsis independent of salicylic acid. Plant Physiol. 2006;142(4):1548–58.
19. Miller MJ, Barrett-Wilt GA, Hua Z, Vierstra RD. Proteomic analyses identify a diverse array of nuclear processes affected by small ubiquitin-like modifier conjugation in Arabidopsis. Proc Natl Acad Sci U S A. 2010;107(38):16512–7.
20. Cohen-Peer R, Schuster S, Meiri D, Breiman A, Avni A. Sumoylation of Arabidopsis heat shock factor A2 (HsfA2) modifies its activity during acquired thermotolerance. Plant Mol Biol. 2010;74(1–2):33–45.
21. Suri SS, Dhindsa RS. A heat-activated MAP kinase (HAMK) as a mediator of heat shock response in tobacco cells. Plant Cell Environ. 2008;31(2):218–26.
22. Liu HT, Gao F, Li GL, Han JL, Liu DL, Sun DY, Zhou RG. The calmodulin-binding protein kinase 3 is part of heat-shock signal transduction in Arabidopsis thaliana. Plant J. 2008;55(5):760–73.

23. Sangwan V, Orvar BL, Beyerly J, Hirt H, Dhindsa RS. Opposite changes in membrane fluidity mimic cold and heat stress activation of distinct plant MAP kinase pathways. Plant J. 2002;31(5):629–38.
24. Waadt R, Seller CA, Hsu PK, Takahashi Y, Munemasa S, Schroeder JI. Plant hormone regulation of abiotic stress responses. Nat Rev Mol Cell Biol. 2022;23(10):680–94.
25. Guo Z, Zuo Y, Wang S, Zhang X, Wang Z, Liu Y, Shen Y. Early signaling enhance heat tolerance in Arabidopsis through modulating jasmonic acid synthesis mediated by HSFA2. Int J Biol Macromol 2024:131256.
26. Peng L, Wan X, Huang K, Pei L, Xiong J, Li X, Wang J. AtPUB48 E3 ligase plays a crucial role in the thermotolerance of Arabidopsis. Biochem Biophys Res Commun. 2019;509(1):281–6.
27. Kuang J, Liu J, Mei J, Wang C, Hu H, Zhang Y, Sun M, Ning X, Xiao L, Yang L. A class II small heat shock protein OsHsp18.0 plays positive roles in both biotic and abiotic defense responses in rice. Sci Rep. 2017;7(1):11333.
28. Kim JH, Lim SD, Jang CS. Oryza sativa heat-induced RING finger protein 1 (OsHIRP1) positively regulates plant response to heat stress. Plant Mol Biol. 2019;99(6):545–59.
29. Kim JH, Lim SD, Jang CS. Oryza sativa drought-, heat-, and salt-induced RING finger protein 1 (OsDHSRP1) negatively regulates abiotic stress-responsive gene expression. Plant Mol Biol. 2020;103(3):235–52.
30. Rauch JN, Tse E, Freilich R, Mok S-A, Makley LN, Southworth DR, Gestwicki JE. BAG3 is a modular, scaffolding protein that physically links heat shock protein 70 (Hsp70) to the small heat shock proteins. J Mol Biol. 2017;429(1):128–41.
31. Zhao Y, Du H, Wang Y, Wang H, Yang S, Li C, Chen N, Yang H, Zhang Y, Zhu Y, et al. The calcium-dependent protein kinase ZmCDPK7 functions in heat-stress tolerance in maize. J Integr Plant Biol. 2021;63(3):510–27.
32. Gao F, Han X, Wu J, Zheng S, Shang Z, Sun D, Zhou R, Li B. A heat-activated calcium-permeable channel–Arabidopsis cyclic nucleotide-gated ion channel 6–is involved in heat shock responses. Plant J. 2012;70(6):1056–69.
33. Peng X, Zhang XN, Li B, Zhao LQ. Cyclic nucleotide-gated ion channel 6 mediates thermotolerance in Arabidopsis seedlings by regulating nitric oxide production via cytosolic calcium ions. BMC Plant Biol. 2019;19(1):368.
34. Wang WX, Zhang JJ, Ai LJ, Wu D, Li B, Zhang LG, Zhao LQ. Cyclic nucleotide-gated Ion channel 6 mediates thermotolerance in seedlings by regulating hydrogen peroxide production cytosolic calcium ions. Front Plant Sci. 2021;12:708672.
35. Katano K, Kataoka R, Fujii M, Suzuki N. Differences between seedlings and flowers in anti-ROS based heat responses of Arabidopsis plants deficient in cyclic nucleotide gated channel 2. Plant Physiol Biochemistry: PPB. 2018;123:288–96.
36. Li S, Zhou X, Chen L, Huang W, Yu D. Functional characterization of Arabidopsis thaliana WRKY39 in heat stress. Mol Cells. 2010;29(5):475–83.
37. Liu ZM, Yue MM, Yang DY, Zhu SB, Ma NN, Meng QW. Over-expression of SlJA2 decreased heat tolerance of transgenic tobacco plants via salicylic acid pathway. Plant Cell Rep. 2017;36(4):529–42.
38. Xu J, Zhang B, Jiang C, Ming F. RceIF5A, encoding an eukaryotic translation initiation factor 5A in Rosa chinensis, can enhance thermotolerance, oxidative and osmotic stress resistance of Arabidopsis thaliana. Plant Mol Biol. 2011;75(1–2):167–78.
39. Han Y, Tang A, Wan H, Zhang T, Cheng T, Wang J, Yang W, Pan H, Zhang Q. An APETALA2 homolog, RcAP2, regulates the number of rose petals derived from stamens and response to temperature fluctuations. Front Plant Sci. 2018;9:481.
40. Wang XK, Huang JL. Experimental principles and techniques of plant physiology and biochemistry. Beijing: Higher Education Press; 2015.
41. Li R, Li Y, Kristiansen K, Wang J. SOAP: short oligonucleotide alignment program. Bioinformatics. 2008;24(5):713–4.
42. Li R, Yu C, Li Y, Lam TW, Yiu SM, Kristiansen K, Wang J. SOAP2: an improved ultrafast tool for short read alignment. Bioinformatics. 2009;25(15):1966–7.
43. Raymond O, Gouzy J, Just J, Badouin H, Verdenaud M, Lemainque A, Vergne P, Moja S, Choisne N, Pont C, et al. The Rosa genome provides new insights into the domestication of modern roses. Nat Genet. 2018;50(6):772–7.
44. Kim D, Paggi JM, Park C, Bennett C, Salzberg SL. Graph-based genome alignment and genotyping with HISAT2 and HISAT-genotype. Nat Biotechnol. 2019;37(8):907–15.
45. Langmead B, Salzberg SL. Fast gapped-read alignment with Bowtie 2. Nat Methods. 2012;9(4):357–9.
46. Li B, Dewey CN. RSEM: accurate transcript quantification from RNA-Seq data with or without a reference genome. BMC Bioinformatics. 2011;12:323.
47. Love MI, Huber W, Anders S. Moderated estimation of Fold change and dispersion for RNA-seq data with DESeq2. Genome Biol. 2014;15(12):550.
48. Kumar L. Mfuzz: a software package for soft clustering of microarray data. Bioinformation. 2007;2(1):5–7.
49. Wen B, Mei ZL, Zeng CW, Liu SQ. metaX: a flexible and comprehensive software for processing metabolomics data. BMC Bioinformatics. 2017;18(1):183.
50. Barker M, Rayens W. Partial least squares for discrimination. J Chemom. 2003;17(3):166–73.
51. Westerhuis JA, Hoefsloot HCJ, Smit S, Vis DJ, Smilde AK, van Velzen EJJ, van Duijnhoven JPM, van Dorsten FA. Assessment of PLSDA Cross validation. Metabolomics. 2008;4(1):81–9.
52. Rohart F, Gautier B, Singh A, KA LC. mixOmics: an R package for 'omics feature selection and multiple data integration. PLoS Comput Biol. 2017;13(11):e1005752.
53. Narusaka M, Shiraishi T, Iwabuchi M, Narusaka Y. The floral inoculating protocol: a simplified Arabidopsis thaliana transformation method modified from floral dipping. Plant Biotechnol-Nar. 2010;27(4):349–51.
54. Lv WT, Lin B, Zhang M, Hua XJ. Proline accumulation is inhibitory to Arabidopsis seedlings during heat stress. Plant Physiol. 2011;156(4):1921–33.
55. Rajametov SN, Yang EY, Cho MC, Chae SY, Jeong HB, Chae WB. Heat-tolerant hot pepper exhibits constant photosynthesis via increased transpiration rate, high proline content and fast recovery in heat stress condition. Sci Rep. 2021;11(1):14328.
56. Kavi Kishor PB, Suravajhala P, Rathnagiri P, Sreenivasulu N. Intriguing role of proline in redox potential conferring high temperature stress tolerance. Front Plant Sci. 2022;13:867531.
57. Cui M, Liang Z, Liu Y, Sun Q, Wu D, Luo L, Hao Y. Flavonoid profile of Anoectochilus Roxburghii (Wall.) Lindl. Under short-term heat stress revealed by integrated metabolome, transcriptome, and biochemical analyses. Plant Physiol Biochemistry: PPB. 2023;201:107896.
58. Jan R, Kim N, Lee SH, Khan MA, Asaf S, Lubna, Park JR, Asif S, Lee IJ, Kim KM. Enhanced flavonoid accumulation reduces combined salt and heat stress through regulation of transcriptional and hormonal mechanisms. Front Plant Sci. 2021;12:796956.
59. Hassan AHA, Hozzein WN, Mousa ASM, Rabie W, Alkhalifah DHM, Selim S, AbdElgawad H. Heat stress as an innovative approach to enhance the antioxidant production in Pseudooceanicola and Bacillus isolates. Sci Rep. 2020;10(1):15076.
60. Netshimbupfe MH, Berner J, Van Der Kooy F, Oladimeji O, Gouws C. Influence of drought and heat stress on mineral content, antioxidant activity and bioactive compound accumulation in four African Amaranthus species. Plants (Basel Switzerland) 2023, 12(4).
61. Cao DD, Li H, Yi JY, Zhang JJ, Che HL, Cao JK, Yang L, Zhu CQ, Jiang WB. Antioxidant properties of the mung bean flavonoids on alleviating heat stress. PLoS ONE. 2011;6(6):e21071.
62. Danquah A, de Zelicourt A, Colcombet J, Hirt H. The role of ABA and MAPK signaling pathways in plant abiotic stress responses. Biotechnol Adv. 2014;32(1):40–52.
63. Hettenhausen C, Schuman MC, Wu J. MAPK signaling: a key element in plant defense response to insects. Insect Sci. 2015;22(2):157–64.
64. Meng X, Zhang S. MAPK cascades in plant disease resistance signaling. Annu Rev Phytopathol. 2013;51:245–66.
65. Smékalová V, Doskočilová A, Komis G, Samaj J. Crosstalk between secondary messengers, hormones and MAPK modules during abiotic stress signalling in plants. Biotechnol Adv. 2014;32(1):2–11.
66. Zhang M, Su J, Zhang Y, Xu J, Zhang S. Conveying endogenous and exogenous signals: MAPK cascades in plant growth and defense. Curr Opin Plant Biol. 2018;45(Pt A):1–10.
67. Wu C, Zhang X, Cui Z, Gou J, Zhang B, Sun X, Xu N. Patatin-like phospholipase A-induced alterations in lipid metabolism and jasmonic acid production affect the heat tolerance of Gracilariopsis Lemaneiformis. Mar Environ Res. 2022;179:105688.
68. Sharma M, Laxmi A. Jasmonates: emerging players in controlling temperature stress tolerance. Front Plant Sci. 2015;6:1129.
69. Balfagón D, Sengupta S, Gómez-Cadenas A, Fritschi FB, Azad RK, Mittler R, Zandalinas SI. Jasmonic acid is required for plant acclimation to a combination of high light and heat stress. Plant Physiol. 2019;181(4):1668–82.
70. Godinho CP, Costa R, Sá-Correia I. The ABC transporter Pdr18 is required for yeast thermotolerance due to its role in ergosterol transport and plasma membrane properties. Environ Microbiol. 2021;23(1):69–80.
71. Takayama S, Xie Z, Reed JC. An evolutionarily conserved family of Hsp70/Hsc70 molecular chaperone regulators. J Biol Chem. 1999;274(2):781–6.
72. Zhang LS, Wu SD, Chang XJ, Wang XY, Zhao YP, Xia YP, Trigiano RN, Jiao YN, Chen F. The ancient wave of polyploidization events in flowering plants

and their facilitated adaptation to environmental stress. Plant Cell Environ. 2020;43(12):2847–56.
73. Yang L, Jin J, Fan D, Hao Q, Niu J. Transcriptome Analysis of Jujube (Ziziphus jujuba Mill.) Response to Heat Stress. *International journal of genomics* 2021, 2021:3442277.
74. Wang TY, Wu JR, Duong NKT, Lu CA, Yeh CH, Wu SJ. HSP70-4 and farnesylated AtJ3 constitute a specific HSP70/HSP40-based chaperone machinery essential for prolonged heat stress tolerance in Arabidopsis. J Plant Physiol. 2021;261:153430.
75. Lee JH, Schöffl F. An Hsp70 antisense gene affects the expression of HSP70/HSC70, the regulation of HSF, and the acquisition of thermotolerance in transgenic Arabidopsis thaliana. Mol Gen Genetics: MGG. 1996;252(1–2):11–9.
76. Jung KH, Gho HJ, Nguyen MX, Kim SR, An G. Genome-wide expression analysis of HSP70 family genes in rice and identification of a cytosolic HSP70 gene highly induced under heat stress. Funct Integr Genomics. 2013;13(3):391–402.
77. Gu LL, Li MZ, Wang GR, Liu XD. Multigenerational heat acclimation increases thermal tolerance and expression levels of Hsp70 and Hsp90 in the rice leaf folder larvae. J Therm Biol. 2019;81:103–9.
78. Jiang C, Bi Y, Zhang R, Feng S. Expression of RcHSP70, heat shock protein 70 gene from Chinese rose, enhances host resistance to abiotic stresses. Sci Rep. 2020;10(1):2445.
79. Li Z, Hartl FU, Bracher A. Structure and function of hip, an attenuator of the Hsp70 chaperone cycle. Nat Struct Mol Biol. 2013;20(8):929–35.
80. Behnam B, Iuchi S, Fujita M, Fujita Y, Takasaki H, Osakabe Y, Yamaguchi-Shinozaki K, Kobayashi M, Shinozaki K. Characterization of the promoter region of an Arabidopsis gene for 9-cis-epoxycarotenoid dioxygenase involved in dehydration-inducible transcription. DNA Res. 2013;20(4):315–24.
81. Zhang Y, Liu X, Su R, Xiao Y, Deng H, Lu X, Wang F, Chen G, Tang W, Zhang G. 9-cis-epoxycarotenoid dioxygenase 1 confers heat stress tolerance in rice seedling plants. Front Plant Sci. 2022;13:1092630.
82. Li B, Jiang S, Gao L, Wang W, Luo H, Dong Y, Gao Z, Zheng S, Liu X, Tang W. Heat shock factor A1s are required for phytochrome-interacting factor 4-mediated thermomorphogenesis in Arabidopsis. J Integr Plant Biol. 2024;66(1):20–35.
83. Chen C, Letnik I, Hacham Y, Dobrev P, Ben-Daniel B-H, Vanková R, Amir R, Miller G. ASCORBATE PEROXIDASE6 protects Arabidopsis desiccating and germinating seeds from stress and mediates cross talk between reactive oxygen species, abscisic acid, and auxin. Plant Physiol. 2014;166(1):370–83.

Publisher's note